

Generation of a novel mouse model that recapitulates early and adult onset glycogenosis type IV

H. Orhan Akman^{1,*}, Tatiana Sheiko¹, Stacey K.H. Tay⁴, Milton J. Finegold², Salvatore DiMauro⁵ and William J. Craigen^{1,3}

¹Department of Molecular and Human Genetics, ²Department of Pathology and ³Department of Pediatrics, Baylor College of Medicine, Houston, TX, USA, ⁴Department of Pediatrics, Yong Loo Lin School of Medicine, National University Health Systems, Singapore and ⁵Department of Neurology, Columbia University Medical Center, New York, NY, USA

Received June 4, 2011; Revised and Accepted August 16, 2011

Glycogen storage disease type IV (GSD IV) is a rare autosomal recessive disorder caused by deficiency of the glycogen branching enzyme (GBE). The diagnostic feature of the disease is the accumulation of a poorly branched form of glycogen known as polyglucosan (PG). The disease is clinically heterogeneous, with variable tissue involvement and age of disease onset. Absence of enzyme activity is lethal *in utero* or in infancy affecting primarily muscle and liver. However, residual enzyme activity (5–20%) leads to juvenile or adult onset of a disorder that primarily affects muscle as well as central and peripheral nervous system. Here, we describe two mouse models of GSD IV that reflect this spectrum of disease. Homologous recombination was used to insert flippase recognition target recombination sites around exon 7 of the *Gbe1* gene and a phosphoglycerate kinase-Neomycin cassette within intron 7, leading to a reduced synthesis of GBE. Mice bearing this mutation (*Gbe1^{neo/neo}*) exhibit a phenotype similar to juvenile onset GSD IV, with wide spread accumulation of PG. Meanwhile, FLPe-mediated homozygous deletion of exon 7 completely eliminated GBE activity (*Gbe1^{-/-}*), leading to a phenotype of lethal early onset GSD IV, with significant *in utero* accumulation of PG. Adult mice with residual GBE exhibit progressive neuromuscular dysfunction and die prematurely. Differently from muscle, PG in liver is a degradable source of glucose and readily depleted by fasting, emphasizing that there are structural and regulatory differences in glycogen metabolism among tissues. Both mouse models recapitulate typical histological and physiological features of two human variants of branching enzyme deficiency.

INTRODUCTION

Glycogen is a highly branched glucose polymer synthesized by two enzymes: (i) glycogen synthase (GYS), which attaches glucose to nascent linear chains of glycogen; and (ii) the glycogen branching enzyme (GBE), which attaches a short branch of approximately 4 glucose units to the linear chain. Absence of GBE causes glycogen storage disease type IV (GSD IV, OMIM 232500). GSD IV is an autosomal recessive disorder typically diagnosed histologically by the accumulation of a poorly branched form of glycogen known as polyglucosan (PG).

In GSD IV, PG mainly accumulates in the liver, heart, skeletal muscles and the central nervous system, tissues with high metabolic activity. GSD IV is a very heterogeneous disorder, affecting different organs at different ages, with visceral and/or neuromuscular involvement. Based upon the amount of residual GBE activity, there are clinically distinguishable forms of the disease, including an early onset form with no residual enzyme activity, a juvenile or adult-onset form associated with partial activity and a clinically distinct adult-onset disease that is known as adult polyglucosan body disease (APBD). The infantile form of the disease is known as Andersen

*To whom correspondence should be addressed at: Department of Molecular and Human Genetics, Baylor College of Medicine, 1 Baylor plaza T528, Houston, TX 77030, USA. Tel: 1 7137988306; Email: hoakman@bcm.edu, hoa2101@columbia.edu or ho_akman@yahoo.com

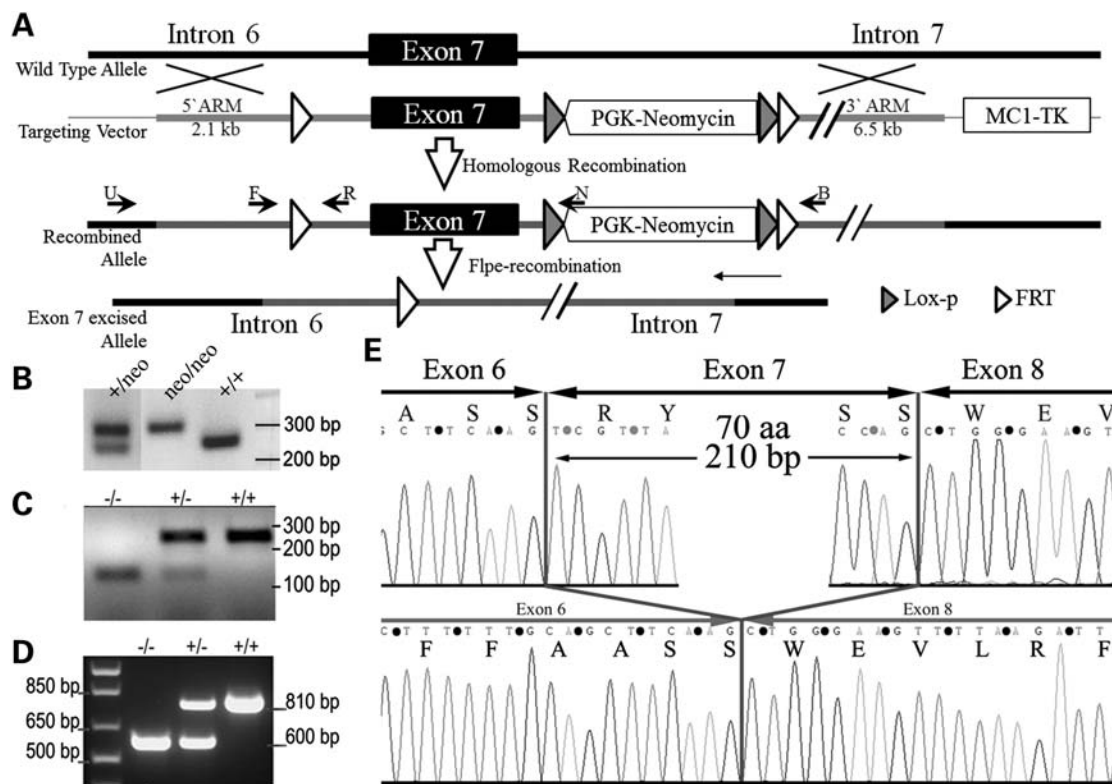


Figure 1. Gene targeting and molecular characterization of a GBE-deficient mouse model. (A) A partial map of the *Gbe1* locus and the targeting vector containing FRT sites flanking exon 7 before and after homologous recombination in ES cells. Crossing *Gbe1*^{+/*FRT*} mice with ROSA 26-flpe mice excises exon 7 from one allele of the *Gbe1* gene by *Flpe* recombinase. Subsequent breeding of heterozygous mice indicated by *Gbe1*^{+/-} creates a *Gbe1* knockout mouse (*Gbe1*^{-/-}). (B) Agarose gel electrophoresis shows the genotyping of PGK-neomycin cassette positive and negative mice, primers used for the PCR are indicated in (A) as F and B. (C) Agarose electrophoresis shows the genotyping of exon 7 knockout, heterozygous and wild-type embryos, the primers used for genotyping are indicated as F, R and B. (D) RT-PCR analysis of the mRNA extracted from neonatal muscle tissue, using primers spanning exons 5–10. (E) The sequence analysis from exons 6–8 from the RT-PCR product shown in (D) from WT (top) and *Gbe1*^{-/-} (bottom) cDNA.

disease and is typically due to the absence of GBE activity. The clinical features include failure to thrive, hepatosplenomegaly and progressive liver cirrhosis, typically leading to death in early childhood (1). The neuromuscular presentation of the disease can be separated into four groups based upon the age at onset: perinatal, presenting as fetal akinesia and perinatal death; congenital, with hypotonia and death in early infancy; childhood, with myopathy and/or cardiomyopathy; and adult, with isolated myopathy or APBD. APBD was first described in 1971 (2), and is characterized clinically by progressive upper and lower motor neuron dysfunction, marked distal sensory loss (mainly in the lower extremities), early neurogenic bladder, cerebellar dysfunction and dementia (3–7). The typical neuropathologic findings are numerous large PG bodies in peripheral nerves, cerebral hemispheres, basal ganglia, cerebellum and spinal cord (5,7,8). Isolated cases of PG myopathy without peripheral nerve involvement have also been described.

Currently, no treatment is available for GSD IV, although liver transplantation has been performed in patients with apparently isolated liver involvement (9). Two naturally occurring animal models of GBE deficiency, American quarter horses and Norwegian forest cats, are not practical laboratory animals (10,11). Therefore, we developed a mouse

model of GBE deficiency in order to better understand the pathogenesis of the disease and to test therapeutic strategies.

RESULTS

Generation of mice lacking GBE

A mouse model of GBE deficiency was generated by introducing flippase recognition target (FRT) recombination sequences upstream and downstream of the mouse *Gbe1* exon 7 via homologous recombination (Fig. 1A). A representative PCR analysis of genotyping is shown in Figure 1B. *Gbe1*^{+/*Neo*} animals were intercrossed to generate *Gbe1*^{neo/neo} mice, or were bred to a *Flpe*-expressing mice strain (*GT(ROSA)*^{26*Sor-Flpe*}) in order to delete the sequences between two FRT sites (represented by the open triangles in Fig. 1A). PCR analysis using primers that bind upstream and downstream of exon 7 amplifies a 160 bp DNA fragment instead of a 3020 bp DNA fragment after deletion of the intervening region containing exon 7 and the phosphoglycerate kinase (PGK)-Neomycin cassette. The third reverse primer located downstream of the 5' FRT site amplifies wild-type DNA in the same PCR reaction in order to detect heterozygous and wild-type litters (Fig. 1C). The resulting heterozygous exon 7-deleted mice (*Gbe1*^{+/-}) were interbred to obtain

homozygous animals. In order to confirm the absence of exon 7, total muscle RNA isolated from newborn litters of *Gbe1*^{+/-} parents was isolated and amplified by reverse transcription-polymerase chain reaction (RT-PCR) analysis. The PCR primers were designed to amplify an 810 bp wild-type *Gbe1* mRNA fragment spanning exons 4–10 that are 54 kb apart in genomic DNA. After FLPe-mediated deletion, a 210 bp long fragment corresponding to exon 7 was absent from the cDNA (Fig. 1D and E). RT-PCR products were sequenced to demonstrate the exact location of the deletion (Fig. 1E).

GBE-deficient embryos are stillborn after a normal gestation

Loss of GBE activity in humans can lead to *in utero* death (12–14). *Gbe1*^{-/-} mice likewise die at or soon after birth. In order to analyze the time of death of *Gbe1*^{-/-} embryos, we performed timed mating of *Gbe1*^{+/-} animals. Litter size and genotype analysis demonstrate that *Gbe1*^{-/-} pups have normal embryonic survival. The mice are comparable to heterozygous and wild-type littermates in terms of size and appearance at E17.5 and after birth (Fig. 2A and B). Ultrasound analysis of E20 pregnant females did not identify any abnormalities in morphology or cardiac function (data not shown). Segregation of the deletion follows the expected Mendelian distribution: out of 49 pups, 12 were wild-type, 24 were heterozygous and 13 homozygous. Western blot analysis of muscle extracts obtained from embryos at E17.5 demonstrated the absence of GBE protein, while *Gbe1*^{+/-} and *Gbe1*^{+/+} animals express detectable GBE protein. In contrast, adult animals harboring the PGK-Neomycin cassette (*Gbe1*^{neo/neo}) had a significantly reduced but still detectable amount of GBE protein in muscle and liver (Fig. 2D). Reduced GBE protein causes early death in homozygous mice. Seventeen recorded deaths were analyzed by MedCalc Software (MedCalc® Version 11.6.1.0 Copyright© 1993–2011) and a Kaplan–Meier curve was plotted (Fig. 2E). No *Gbe1*^{neo/neo} mice survived beyond 39 weeks.

Effect of the absence GBE on glycogen content

We measured GBE activity in E17.5 embryonic muscle tissue. There was no detectable GBE activity in the *Gbe1*^{-/-} tissue (Table 1), while *Gbe1*^{neo/neo} animals had a low but detectable amount of GBE activity (Table 2). Next, we determined the glycogen content in muscle tissue from the different genotypes. *Gbe1*^{-/-} mice had a significantly reduced amount of measurable glycogen. However, in all *Gbe1*^{neo/neo} mice, examined muscle and liver glycogen content was significantly greater than in the controls, reflecting a greater accumulation of the abnormal PG. While the differences in glycogen content between *Gbe1*^{-/-} and *Gbe1*^{neo/neo} mice may simply reflect the time required to accumulate PG, it prompted us to determine the GYS activity and protein levels in the fetal and adult skeletal muscle samples. GYS activity can be measured with or without glucose 6-phosphate, which is a strong allosteric activator of GYS. Surprisingly, higher GYS activity was observed in *Gbe1*^{-/-} muscle relative to that of controls when the assay reaction lacked glucose 6-phosphate. However, in the presence of 10 mM glucose 6-phosphate, the GYS activity in *Gbe1*^{-/-} skeletal muscle failed to match

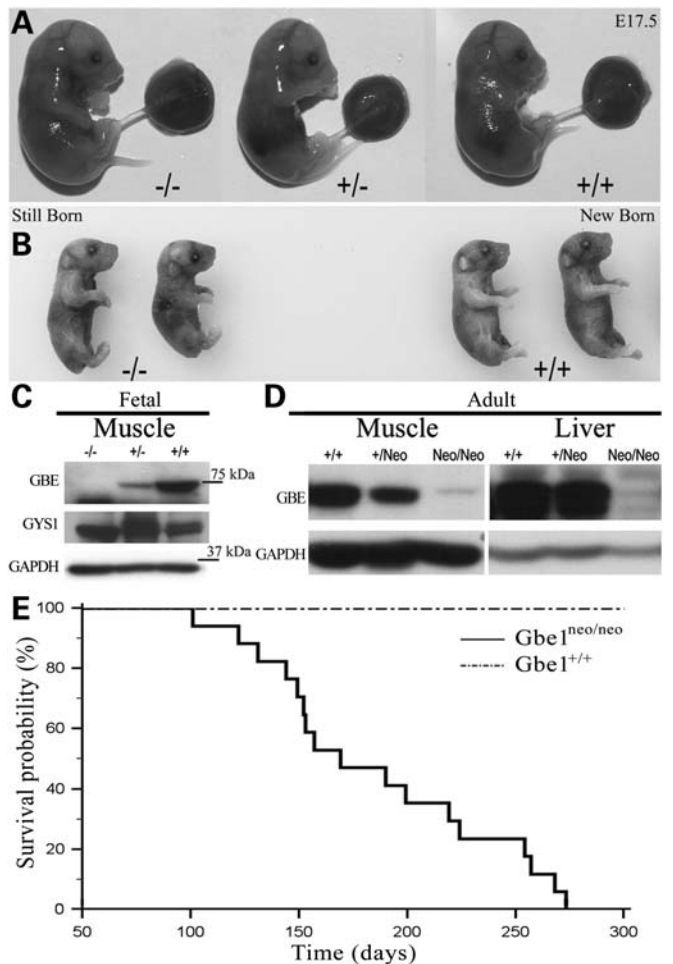


Figure 2. Lack of GBE does not affect embryonic development. (A) Embryos at E17.5. *Gbe1*^{-/-}, *Gbe1*^{+/-} and *Gbe1*^{+/+}, indicated by -/-, +/- and +/+. Note no evidence of hydrops fetalis. (B) Stillborn *Gbe1*^{-/-} and *Gbe1*^{+/+} neonates from the same litter are shown after being genotyped and fixed in 10% formalin. (C) Western blot analysis of GBE and GYS1 in muscle extracts obtained from *Gbe1*^{-/-}, *Gbe1*^{+/-} and *Gbe1*^{+/+} embryos shown in (A). (D) Western blot analysis of GBE in adult muscle and liver tissue of *Gbe1*^{+/+}, *Gbe1*^{+/Neo} and *Gbe1*^{neo/neo}. (E) Kaplan–Meier plot illustrates the incidence of death in *Gbe1*^{neo/neo} versus *Gbe1*^{+/+} mice. $P < 0.0001$, $n = 17$.

Table 1. Muscle glycogen content, GBE and GS activity

	Glycogen content w/w	GBE activity (nmol/min/mg)	GS activity (nmol/min/mg)	
			Without G6P	With G6P
<i>Gbe1</i> ^{-/-}	0.8 ± 1.6*	0 ± 2*	26 ± 1.8*	44 ± 1.0*
<i>Gbe1</i> ^{+/-}	13.1 ± 3.13	153 ± 17	17 ± 3.2	68 ± 3.1
<i>Gbe1</i> ^{+/+}	10.5 ± 1.5	227 ± 44	19 ± 1.0	69 ± 1.4

Values represent the Mean ± SD, * $P < 0.01$ *Gbe1*^{-/-} ($n = 5$) versus both *Gbe1*^{+/-} ($n = 4$) and *Gbe1*^{+/+} ($n = 5$).

the enhanced GYS activity seen in *Gbe1*^{+/-} and *Gbe1*^{+/+} samples. As indicated in Table 1, the maximal activity of GYS was significantly lower than in control and heterozygous littermates, and the difference in responsiveness to glucose 6-phosphate likely reflects additional as yet unknown regulatory

Table 2. Tissue GBE activity in wild-type and *Gbe1^{neo/neo}* deficient mice

	<i>Gbe1^{+/+}</i>	<i>Gbe1^{neo/neo}</i>	Percent change
Brain	230 ± 17	25 ± 8	11%
Heart	457 ± 56	72 ± 34	16%
Liver	855 ± 43	115 ± 42	13%
Kidney	497 ± 43	ND	
Muscle	251 ± 23	38 ± 18	15%

Values represent the mean ± SD, $P < 0.001$ ($n = 6$ for each group); ND, not detected.

changes to GYS in the absence of GBE activity. Western blotting revealed comparable amounts of GYS1 protein in all three genotypes (Fig. 2C); *Gbe1^{-/-}* neonates contain detectable PG. We determined whether glycogen is present in other fetal tissues. Due to size limitations, we used whole-mount embryo sections and assessed the glycogen content by histochemistry. Whole embryos were fixed in 10% buffered formaldehyde and sections were stained with Periodic Schiff base (PAS). Before PAS staining, the slides were either untreated or treated with diastase (alpha amylase). Limited digestion with diastase degrades almost all structurally normal glycogen, while longer and poorly branched PG remains intact and thus stains with PAS. Whole cross-sections were examined by light microscopy and vacuoles in the control neonatal liver can be seen (Fig. 3A), where glycogen was present. In contrast, *Gbe1^{-/-}* liver lacked any significant vacuoles, reflecting an overall reduction in glycogen, but a detectable accumulation of PG (Fig. 3B). Similarly, following diastase digestion, glycogen was absent from intercostal muscles of *Gbe^{+/+}* newborn pups (Fig. 3C), but PG was readily observed in *Gbe1^{-/-}* animals (Fig. 3D). In the heart, *Gbe^{-/-}* newborn pups exhibited extensive vacuolization (Fig. 3F and H) in comparison to control mice (Fig. 3E and G), and there was widespread and prominent PG accumulation (Fig. 3H).

Low GBE activity leads to PG formation in tissues

Clinically, GSD IV is diagnosed by the presence of poorly branched glycogen that is resistant to diastase digestion. Therefore, we examined the accumulation of diastase-resistant PG in multiple organs from 4-month-old *Gbe1^{neo/neo}* mice. The juvenile and adult form of GSD IV is typically a neuromuscular disorder, therefore brain and muscle samples were examined first. Brain sections of *Gbe1^{neo/neo}* mice had PG bodies located in the somas and extended processes of neurons (Fig. 4A and B). Skeletal muscle and heart sections also showed PG bodies, which were absent in normal muscle and heart (Fig. 4C–F).

Liver stores glucose in the form of glycogen and uses it to maintain blood glucose levels between meals, therefore liver tissue was examined for the accumulation of PG, and there was a significant amount of PG following diastase digestion compared with control sections (Fig. 4G and H). However, a similar PG accumulation was not observed in smooth muscle, kidney or spleen sections (Supplementary Material, Figure).

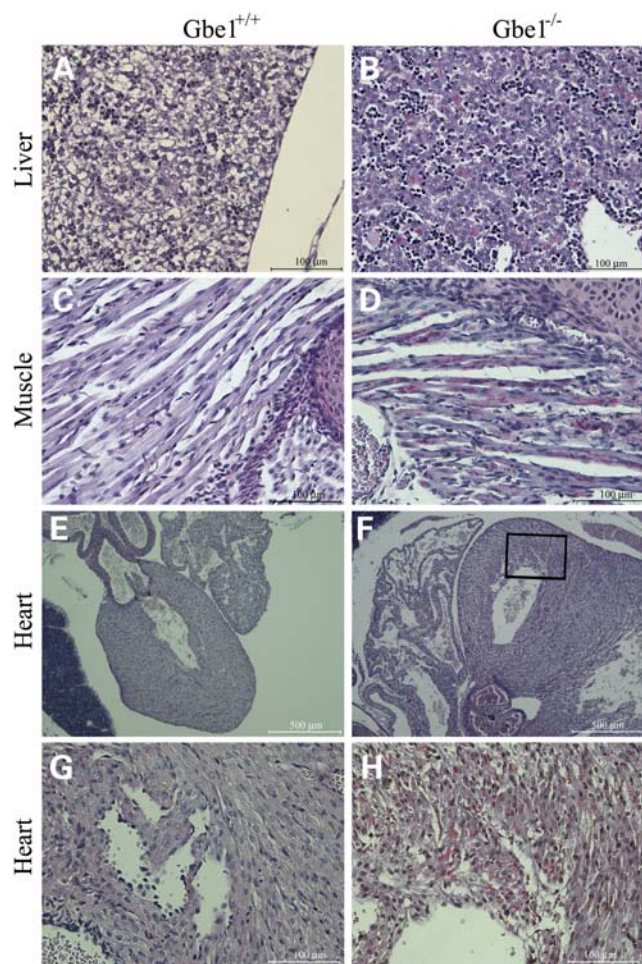


Figure 3. *Gbe1^{-/-}* newborns accumulate abnormal glycogen in multiple tissues. Formalin-fixed, paraffin-embedded sections of whole mouse newborns digested with diastase and PAS stained for glycogen. Control (A) and *Gbe1^{-/-}* (B) liver sections, note the reduction in cleared areas in the *Gbe1^{-/-}* liver, reflecting reduction in total glycogen content, while also accumulating PG ($\times 400$ magnification). Intercostal muscles control (C) and *Gbe1^{-/-}* (D) mice ($\times 400$ magnification), note the red stained PG. Control (E) and *Gbe1^{-/-}* (F) heart sections ($\times 40$ magnification); boxed area ($\times 400$ magnification) from the *Gbe1^{-/-}* tissue exhibits widespread vacuolization and extensive PG accumulation in comparison to the control (G and H).

Accumulated PG is not membrane-bound

Heart and skeletal muscle samples were prepared and examined by electron microscopy. Heart and skeletal muscle images show PG bodies of 1 and 5 μm size, respectively. Magnified images clearly show that PG is not membrane-bound but free in the cytosol, both in skeletal muscle and heart (Fig. 5A and B).

Glucose metabolism is subtly altered in *Gbe1^{neo/neo}* mice

A defect in synthesizing normal glycogen and degrading abnormal PG may be expected to interfere with normal glucose uptake and release. Therefore, adult *Gbe1^{neo/neo}* animals were assessed for their ability to store and mobilize glucose efficiently by glucose tolerance testing. Figure 6

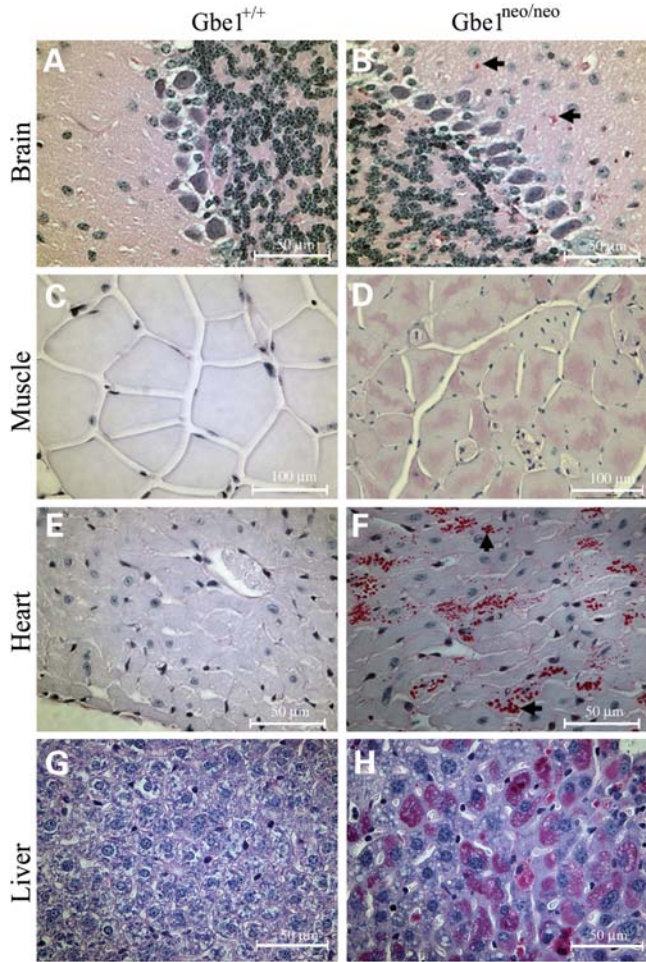


Figure 4. Decreased GBE activity leads to widespread PG accumulation. PG (red stain) is detected in brain, heart, skeletal muscle and liver sections from *Gbe1^{neo/neo}* mice. Images are $\times 400$ magnification, except for muscle sections photographed at $\times 200$ magnification.

shows that *Gbe1^{neo/neo}* animals were mildly hypoglycemic after a 16 h fast compared with controls. After glucose administration, peak blood glucose values in *Gbe1^{neo/neo}* animals were similar to controls, but glucose values returned to baseline in < 90 min in *Gbe1^{neo/neo}* mice, while in the control animals blood glucose decreased more gradually over a 3 h period.

Catabolism of PG is different in *Gbe1^{neo/neo}* liver than in muscle and other tissues

The rapid absorption of glucose and slightly lower blood glucose levels raised the question of whether the liver in *Gbe1^{neo/neo}* animals can adequately degrade PG that has been formed during feeding. Animals were fasted for 16 h and muscle and liver glycogen content assessed by biochemical analysis. The quality of glycogen was tested by PAS staining after diastase digestion. Glycogen levels were quantified as percent glucose weight by wet tissue weight (w/w) (Fig. 7A). Before fasting, *Gbe1^{neo/neo}* animals have significantly higher glycogen content in liver and muscle in comparison to control animals. After fasting for 16 h, muscle glycogen

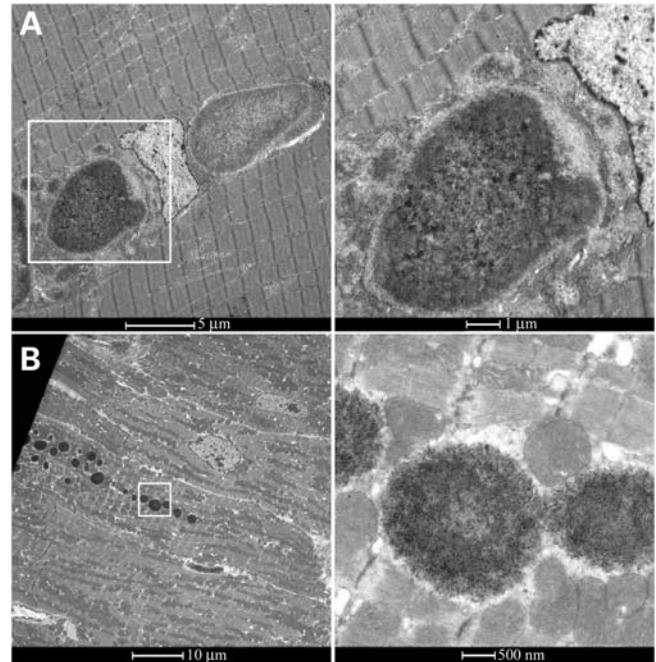


Figure 5. PG is not membrane-bound in skeletal muscle and cardiac myofibers. Transmission electron micrograph showing the ultra structure of PG in skeletal muscle (A) and heart (B). Two micrographs on the right show the framed areas in higher magnification [$10\times$ (top) and $20\times$ (bottom) fold].

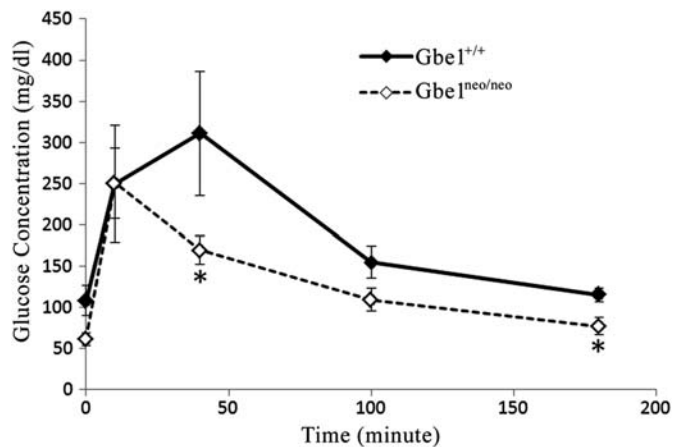


Figure 6. *Gbe1^{neo/neo}* mice have lower blood glucose levels before and after a glucose challenge. Glucose tolerance curves in wild-type (diamond) and GBE-deficient (square) groups ($n = 6$ for each group). Error bars for the different time point values represent the mean \pm SD, $P < 0.01$ where indicated (*).

content did not change in *Gbe1^{neo/neo}* mice, while control animals had significantly lower muscle glycogen content, reflecting the degradation of muscle glycogen. However, liver glycogen content decreased significantly in *Gbe1^{neo/neo}* animals after fasting, indicating that, unlike muscle, *Gbe1^{neo/neo}* liver utilized PG during fasting. Histological analysis of liver confirmed the accumulation and degradation of PG (Fig. 7B), whereas muscle and heart sections demonstrate significant amounts of PG even after fasting.

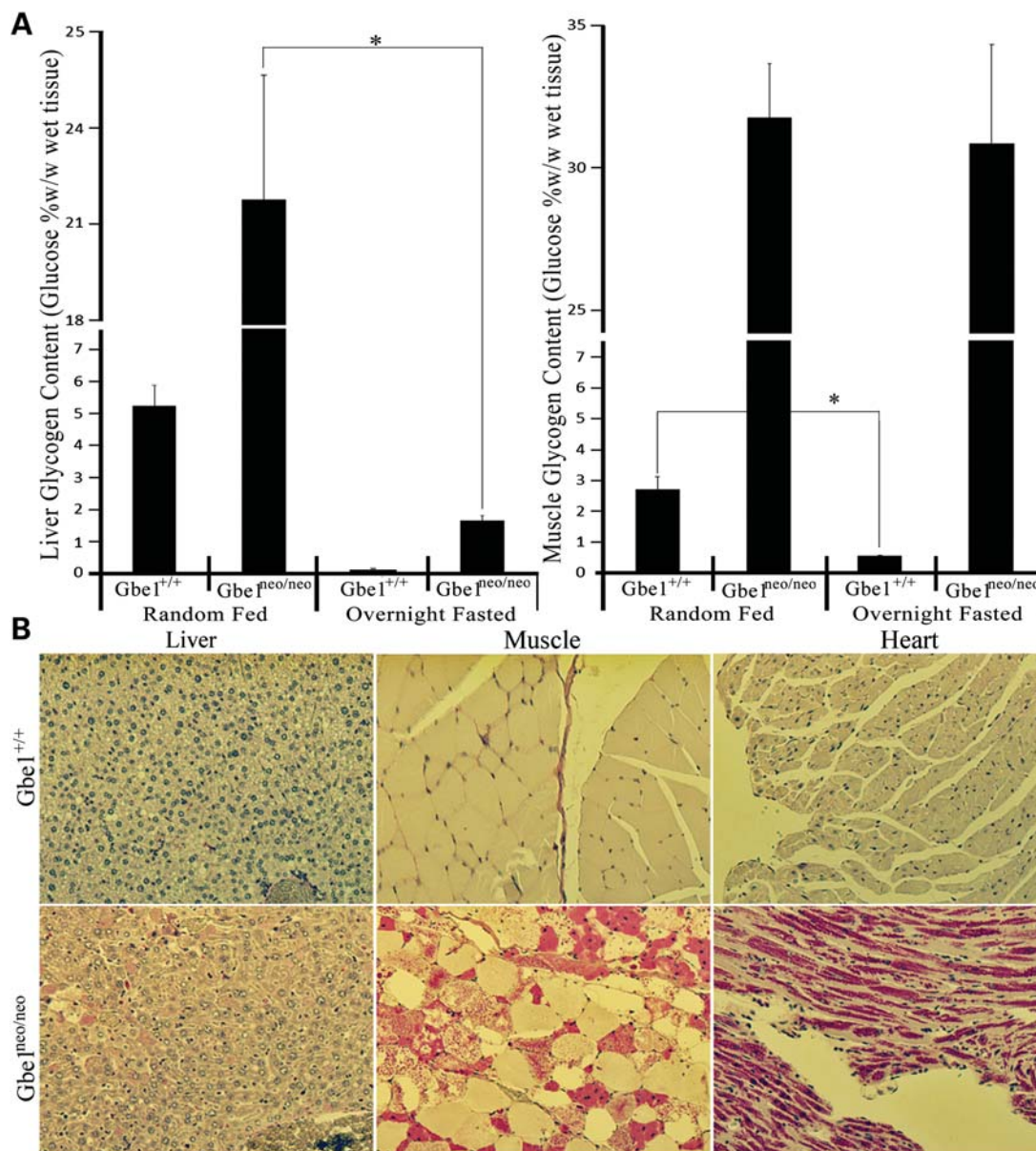


Figure 7. GBE-deficient liver can degrade PG during fasting. (A) Liver and muscle glycogen content in wild-type and *Gbe1*^{neo/neo} animals was measured before and after a 16 h fast ($n = 5$ for each treatment). Glycogen content is expressed as percent glucose w/w in fresh tissue. Error bars represent the mean \pm SD, $P < 0.001$ where indicated (*). (B) Diastase treated and PAS stained liver, skeletal muscle and heart sections from the 16 h fasted wild-type and *Gbe1*^{neo/neo} mice.

DISCUSSION

GBE deficiency is a rare disorder with a very heterogeneous clinical presentation that appears to be determined in part by the degree of residual enzyme activity. Complete loss of activity in humans is lethal either in the third trimester of pregnancy or in infancy, while mutations that reduce enzyme activity cause juvenile or adult-onset disease. Juvenile onset disease typically exhibits liver and/or heart involvement, while adult-onset disease is mainly a neuromuscular disorder and may be misdiagnosed as amyotrophic lateral sclerosis, multiple sclerosis or Alzheimer disease (5,7,15). Here we describe a mouse model of GSD IV that accurately recapitulates *histological* this disease spectrum. Deletion of exon 7 eliminates enzyme activity

in all tissues and thus is a model of Andersen disease. In contrast, decreasing the expression of the *Gbe1* via transcriptional interference by the reverse-oriented PGK-Neomycin cassette leads to a hypomorphic allele with residual enzyme activity and later onset of disease, yet a pronounced accumulation of PG. Exon 7 of *Gbe1* contains the c-terminus of the alpha amylase domain and the linker region that connects the alpha amylase domain to the glycosyl transferase domain. Since exon 7 encodes an in-frame 70-amino acid polypeptide, its deletion may potentially lead to an internally truncated protein. Unfortunately, our western blot result does not show the shorter predicted protein due to a cross-reacting band that obscures the predicted size. Removal of exon 7 *in vivo* by FLPE-mediated recombination leads to *Gbe1*^{-/-} pups that die at birth. *In*

utero development appears unaffected by the mutation. While total glycogen content is reduced in all tissues, a significant amount of PG is present. This finding is in contrast to that reported recently by Lee *et al.* (13), where a nonsense mutation in *Gbe1* was identified following random chemical mutagenesis. The authors reported little accumulation of PG, and attributed the embryonic lethality that was observed to a developmental heart defect (ventricular non-compaction) and fetal hydrops, findings we have not observed. This difference may reflect strain-specific differences, or, perhaps less likely, a second linked mutation present in the mutagenized strain studied. The absence of significant amounts of PG in the strain reported by Lee *et al.* is in contrast to the observed accumulation of PG in postmortem human embryos harboring large homozygous deletions or point mutations that are predicted to eliminate GBE activity (16). In these human cases, PG accumulated in vital organs such as the brain stem and the sympathetic and parasympathetic nervous system that control postnatal respiration.

Normally, glycogen is found in fetal skeletal muscle, liver and heart, as shown in the PAS staining of whole-mount wild-type E17.5 embryo sections. This demonstrates that there is fetal glycogen synthesis and thus GYS activity that would be required to initiate glycogen synthesis. This fetal glycogen is stored to be used during delivery and after birth in order to provide glucose until newborns begin feeding. With this in mind, we studied the GYS activity in embryos. GYS is under both hormonal and allosteric regulation by glucose-6 phosphate. Allosteric regulation is believed to supersede the hormonal inhibition mediated by phosphorylation, so as to protect the cell against very high intracellular glucose concentrations. High intracellular glucose causes glycogen accumulation irrespective of cellular energy status, as demonstrated in disorders of glycolysis, where, despite a metabolic block in glycolysis that causes an intracellular energy deficit, glycogen still accumulates (17,18). We have found substantial GYS activity in *Gbe1*^{-/-} skeletal muscle and abundant GYS protein. However, GYS activity in *Gbe1*^{-/-} mice is considerably less responsive to glucose 6-phosphate-mediated activation in comparison to that of control mice, suggesting that there is a minimal requirement for GBE in the allosteric activation of GYS. Lack of glycogen in tissues in the absence of GYS has been reported previously (19,20). Unlike GBE, GYS has two isoforms; liver-specific GYS2 and GYS1 that is expressed in other tissues. GYS2-deficient mice have near-normal development, whereas 90% of GYS1-deficient mice die after birth. Thus, given that there is a single *Gbe1* locus, *Gbe1*^{-/-} mice mimic the course of GYS1-deficient mice, yet, like GYS2-deficient mice, also lack significant amounts of liver glycogen (but readily detectable PG). Hence, the early death of GBE-deficient mice is likely not solely a consequence of an absence of structurally normal glycogen in the liver. While we did not observe hydropic embryos or left ventricular non-compaction, the hearts of *Gbe1*^{-/-} mice appear to have disrupted myocardial architecture in association with widespread PG accumulation. Future studies in *Gbe1*^{-/-} mice will address the molecular basis for this structurally abnormal myocardium.

The PGK-Neomycin cassette used for positive selection in mouse embryonic stem (ES) cells alters the expression of *Gbe1*. Both GBE activity assays and western blotting have shown that transcription of the *Gbe1* gene has been reduced.

This has generated a phenotype similar to the juvenile and adult forms of GSD IV. Point mutations that decrease enzyme activity such as Y329S and R545H cause amylopectinosis as a recessive trait. Thus, in order to manifest the disease, enzyme activity must be <50% (21). However, there are rare case reports of manifesting heterozygotes, with clinical features occurring in the sixth decade of life (22). In aged humans and animals, PG-like bodies known as corpora amylacea can be seen in white matter and axons, but the relationship to GBE activity remains unexplored (23–26). *Gbe1*^{+/-} mice will be aged to determine whether a reduction in GBE can lead to the formation of PG bodies in the brain.

PG is also a component of the Lafora bodies that lead to progressive myoclonus epilepsy [Lafora disease (LD)]. Lafora disease is an autosomal recessive disorder that becomes symptomatic in teenage years, with progressive myoclonic epilepsy leading to death within a decade. LD are found in the pericarya of neurons and other cell types. The pathogenic mechanism of Lafora disease does not involve the glycogenolytic enzymes *per se*, but is caused by the functional loss of regulatory enzymes that may indirectly affect glycogenolytic enzymes (27). Two genes causing LD, *EPM2A* and *NHLRC1* (*EPM2B*), have been identified (28,29). An animal model of LD has been described; however, the exact mechanism of PG formation is not fully understood (30–32). Thus, breeding GBE-deficient mice to LD mice would explore the role of GBE in the pathogenesis of LD.

Gbe1^{neo/neo} mice tolerate fasting and respond to a glucose bolus in a near normal manner, suggesting that storage of glucose as glycogen or PG can occur very efficiently, even with low GBE activity. However, there is a tissue-specific difference in the ability to degrade PG, as reflected by the persistence of muscle PG after fasting, in contrast to its depletion in liver. The loss of PG from the liver belies the common belief that PG is an inert indigestible molecule and suggests that differences between hepatic phosphorylase and myophosphorylase may account for this observation. We found that PG can be degraded in liver but not in other tissues. Further studies will be necessary to compare glycogen breakdown in muscle of *Gbe1*^{Neo/Neo} mice not only after fasting, but also after exercise, and after a combination of the two conditions.

These results raise the possibility of treatment strategies that enhance the physiologic degradation of PG. Therefore, this mouse model will serve as a useful tool for examining the biology of PG formation and its degradation, and as a means for testing possible therapeutic approaches.

MATERIALS AND METHODS

Targeting of *Gbe1*

The *Gbe1* targeting vector was assembled by PCR-amplified and restriction enzyme-digested fragments from ES 129Sv mouse DNA. A 1020 bp *NheI* fragment containing Exon 7 was cloned and modified by inserting FRT oligos upstream and downstream of exon 7. A PGK promoter-Neomycin resistance cassette flanked by loxP sites was cloned 5' to the FRT site downstream of seventh exon for positive drug selection. The final construct contained a 2.1 kb 5'-short recombination arm composed of a portion of intron 6, the upstream FRT

site followed by exon 7, the PGK-Neomycin resistance cassette for positive selection flanked by loxP sites and the FRT site on the 3' end, followed by a 6.5 kb long recombination arm spanning intron 7. Finally, a MC1-driven thymidine kinase-1 gene was incorporated into the plasmid for negative selection against non-homologous recombination (Fig. 1). All of the junctions in the final construct were confirmed by sequencing and restriction enzyme digestion. The *NotI* linearized vector was electroporated into AB2.2 ES cells by the mouse transgenic core facility at Baylor College of Medicine Houston, TX. Selection of ES cells used Ganciclovir[®] as a negative selection drug and G418 for positive selection. Cells surviving in the presence of G418 were screened by PCR for appropriately targeted integration. Positive ES cell clones were confirmed by additional PCR and Southern analyses to contain the two FRT sites to be correctly targeted at both the 5'- and 3'-ends of exon 7. These ES cells were used to generate chimeric mice by blastocyst microinjection and these mice bred to confirm transmission of the targeted allele.

Genotyping wild-type and cre recombined alleles

Tail DNA was isolated by standard techniques and the Gbe1 locus PCR amplified using primers, 5'-AGC TTT GGT TAT AGA CGA ATC ACT, b, 5'-GTC TAT GTC CAG CAC AGT ATT AAG GA and c.-5'-TCC TGA AAT GGG ATA TAT GGG ATA TG. PCR reaction was prepared as described in the vendor's protocol (New England BioLabs). Thermal cycles were programmed for touchdown PCR as follows; initial 5 min denaturation at 95°C followed by touchdown PCR cycles with the following steps; denaturation at 95°C for 30 min, annealing at 65°C decreasing 0.5°C every cycle for the next 20 cycles and 72°C extension. After the touchdown protocol, 20 cycles of regular PCR were carried out starting with 95°C denaturation for 30 s, annealing at 55°C for 30 s and primer extension at 72°C for 45 s. Amplified fragments are separated on 2% agarose gel and photographed.

Glucose tolerance testing

Mice from control and GBE-deficient groups were fasted for 16 h. D-Glucose (1.2 mg/g weight) was injected into the peritoneum of conscious mice. Blood was obtained from the tail at 0, 10, 40, 100 and 180 min after injection, and the glucose concentration was determined with an Elite glucose meter (Glucometer Elite, Bayer).

Preparation of samples for biochemical analyses

Four to 6 months old adult animals and 4-month-old female mice on the 17th day of pregnancy were anesthetized by IsoThesia[™] (Butler Animal Health Supply, Dublin, OH, USA) inhalation and sacrificed by cervical dislocation. The embryos and the tissues of adult animals were immediately frozen in liquid nitrogen and stored at -80°C for further analyses. Tissues were cut, weighed and homogenized in the assay buffers as described below.

Western analysis

For western analysis, a 30 µg of tissue homogenate was subjected to sodium dodecyl sulfate-polyacrylamide gel electrophoresis. Proteins were transferred to nitrocellulose membranes and incubated with monoclonal antibodies raised against human GBE and GYS1 (Origene, Rockville, MD, USA). Detection was achieved with horseradish peroxidase-conjugated secondary antibodies and enhanced chemiluminescence.

Quantification of glycogen

Glycogen content was estimated by measuring glucose released by amyloglucosidase digestion of ethanol-precipitated glycogen from muscle or liver tissue, as described (33). Samples of frozen muscle and liver tissue (~30–60 mg) were boiled in 200 µl of 30% (wt/vol) KOH for 30 min with occasional shaking. After cooling, 67 µl of 0.25 M Na₂SO₄ and 535 µl of ethanol were added. Next, samples were centrifuged at 14 500g for 20 min at 4°C to collect glycogen. The glycogen pellet was suspended in water (100 µl), 200 µl of ethanol was added and centrifugation as described above was used to harvest glycogen. This ethanol precipitation step was repeated, and the glycogen pellet was dried in a Speed-Vac. Dried glycogen pellets were suspended in 100 µl of amyloglucosidase [0.3 mg/ml in 0.2 M sodium acetate (pH 4.8)] and incubated at 37°C for 3 h to digest glycogen. To determine the glucose concentration in the samples, an aliquot (5 µl) of digested glycogen was added to 95 µl of a solution containing 0.3 M triethanolamine (pH 7.6), 0.4 mM MgCl₂, 0.9 mM NADP, 1 mM ATP and 0.1 µg of glucose-6-phosphate dehydrogenase/ml. The absorbance at 340 nm was read before and after the addition of 0.1 µg of hexokinase.

GBE activity

GBE activity was assayed as described by Tay *et al.* (14). Briefly, frozen tissue samples were homogenized in all-glass homogenizers in nine volumes of 5 mM Tris, 1 mM ethylene diamine tetra acetic acid (EDTA), 5 mM mercaptoethanol, pH 7.2 and centrifuged at 9200g for 10 min. Branching enzyme activity was measured by an indirect assay based on incorporation of radioactive glucose-1-phosphate (PerkinElmer Life and Analytical Sciences, Boston, MA, USA) into glycogen by the reverse activity of phosphorylase a (Sigma, St Louis, MO, USA) as an auxiliary enzyme. At 30, 45 and 60 min time intervals, 5 µl of reaction mix was spotted on Whatman[®] Number 5 qualitative filter paper (Maidstone, UK). Unincorporated glucose-1-phosphate was washed for 15 min using three changes of 66% v/v ethanol. Glycogen bound radioactive glucose-1-phosphate was quantified by liquid scintillation counter (Packard Instruments, Boston, MA, USA).

GYS activity

GYS activity was measured as described (18). Briefly, 15 µg muscle extracts homogenized in cold homogenization buffer (50 mM Tris Acetate, pH 7.8, 20 mM NaF and 2 mM EDTA)

was incubated 20 and 40 min in assay buffer (4% glycogen, 10 mM UDP-glucose, ^{14}C labeled UDP-Glucose, 50 mM Tris-HCl pH 7.8 and with or without 10 mM Glucose 6-phosphate). Ten microliters of the reaction mix were spotted at each time point onto Whatman® Number 5 qualitative filter paper, and the filter papers washed and quantified as described in the GBE assay protocol.

Tissue staining and histochemistry

Tissue sections were prepared from 4-month-old mice, fixed in 10% formalin and embedded in paraffin. Slices of 5 μm were deparaffinized, and one slide of each sectioned block was treated with 40 ml of 5 $\mu\text{g}/\text{ml}$ α -Amylase (Sigma) for 25 s in a microwave oven set to 600 watts; slides, washed with deionized water and oxidized with 0.5% periodic acid for 5 min, stained with Schiff reagent for 15 min and then counterstained in hematoxylin for 15 min and rinsed in tap water. The slides were then examined by light microscopy (Nikon Eclipse90i, Melville, NY, USA).

SUPPLEMENTARY MATERIAL

Supplementary Material is available at *HMG* online.

ACKNOWLEDGEMENTS

Our thanks to Doraine Rudman, Pamela Parson and Jim Barrish at Texas Children's Hospital and Bilqees Bhatti in the BCM Comparative Pathology Laboratory for technical assistance.

Conflict of Interest statement. None declared.

FUNDING

This work was supported by a Muscular dystrophy Association Development Grant (MDA10027); the Adult Polyglucosan Body Research Foundation (APBDRF); and the Intellectual and Developmental Disabilities Research Center and Digestive Diseases Center at Baylor College of Medicine. The IDDRC is funded by award number P30HD024064 from the NICHD. The content is solely the responsibility of the authors and does not necessarily represent the official views of the Eunice Kennedy Shriver NICHD or HHH.

REFERENCES

- Andersen, D.H. (1956) Familial cirrhosis of the liver with storage of abnormal glycogen. *Lab. Invest.*, **5**, 11–20.
- Suzuki, K., David, E. and Kutschman, B. (1971) Presenile dementia with 'Lafora-like' intraneuronal inclusions. *Arch. Neurol.*, **25**, 69–80.
- Cafferty, M.S., Lovelace, R.E., Hays, A.P., Servidei, S., Dimauro, S. and Rowland, L.P. (1991) Polyglucosan body disease. *Muscle Nerve*, **14**, 102–107.
- Gray, F., Gherardi, R., Marshall, A., Janota, I. and Poirier, J. (1988) Adult polyglucosan body disease (APBD). *J. Neuropathol. Exp. Neurol.*, **47**, 459–474.
- McDonald, T.D., Faust, P.L., Bruno, C., DiMauro, S. and Goldman, J.E. (1993) Polyglucosan body disease simulating amyotrophic lateral sclerosis. *Neurology*, **43**, 785–790.
- Peress, N.S., DiMauro, S. and Roxburgh, V.A. (1979) Adult polysaccharidosis. Clinicopathological, ultrastructural, and biochemical features. *Arch. Neurol.*, **36**, 840–845.
- Robitaille, Y., Carpenter, S., Karpati, G. and DiMauro, S.D. (1980) A distinct form of adult polyglucosan body disease with massive involvement of central and peripheral neuronal processes and astrocytes: a report of four cases and a review of the occurrence of polyglucosan bodies in other conditions such as Lafora's disease and normal ageing. *Brain*, **103**, 315–336.
- Robertson, N.P., Wharton, S., Anderson, J. and Scolding, N.J. (1998) Adult polyglucosan body disease associated with an extrapyramidal syndrome. *J. Neurol. Neurosurg. Psychiatry*, **65**, 788–790.
- Ban, H.R., Kim, K.M., Jang, J.Y., Kim, G.H., You, H.W., Kim, K., Yu, E., Kim, D.Y., Kim, K.H., Lee, Y.J. *et al.* (2009) Living donor liver transplantation in a Korean child with glycogen storage disease type IV and a GBE1 mutation. *Gut. Liver*, **3**, 60–63.
- Fyfe, J.C., Giger, U., Van Winkle, T.J., Haskins, M.E., Steinberg, S.A., Wang, P. and Patterson, D.F. (1992) Glycogen storage disease type IV: inherited deficiency of branching enzyme activity in cats. *Pediatr. Res.*, **32**, 719–725.
- Valberg, S.J., Ward, T.L., Rush, B., Kinde, H., Hirasagi, H., Nahey, D., Fyfe, J. and Mickelson, J.R. (2001) Glycogen branching enzyme deficiency in quarter horse foals. *J. Vet. Intern. Med.*, **15**, 572–580.
- Bruno, C., van Diggelen, O.P., Cassandrini, D., Gimpelev, M., Giuffrè, B., Donati, M.A., Introvini, P., Alegria, A., Assereto, S., Morandi, L. *et al.* (2004) Clinical and genetic heterogeneity of branching enzyme deficiency (glycogenosis type IV). *Neurology*, **63**, 1053–1058.
- Lee, Y.C., Chang, C.J., Bali, D., Chen, Y.T. and Yan, Y.T. (2010) Glycogen-branching enzyme deficiency leads to abnormal cardiac development: novel insights into glycogen storage disease IV. *Hum. Mol. Genet.*, **20**, 455–465.
- Tay, S.K., Akman, H.O., Chung, W.K., Pike, M.G., Muntoni, F., Hays, A.P., Shanske, S., Valberg, S.J., Mickelson, J.R., Tanji, K. *et al.* (2004) Fatal infantile neuromuscular presentation of glycogen storage disease type IV. *Neuromuscul. Disord.*, **14**, 253–260.
- Abel, T.J., Hebb, A.O., Keene, C.D., Born, D.E. and Silbergeld, D.L. (2010) Parahippocampal corpora amylacea: case report. *Neurosurgery*, **66**, E1206–E1207.
- Taratuto, A.L., Akman, H.O., Saccoliti, M., Riudavets, M., Arakaki, N., Mesa, L., Sevlever, G., Goebel, H. and Dimauro, S. (2010) Branching enzyme deficiency/glycogenosis storage disease type IV presenting as a severe congenital hypotonia: muscle biopsy and autopsy findings, biochemical and molecular genetic studies. *Neuromuscul. Disord.*, **20**, 783–790.
- Baskaran, S., Roach, P.J., DePaoli-Roach, A.A. and Hurley, T.D. (2010) Structural basis for glucose-6-phosphate activation of glycogen synthase. *Proc. Natl Acad. Sci. USA*, **107**, 17563–17568.
- McCue, M.E., Valberg, S.J., Miller, M.B., Wade, C., DiMauro, S., Akman, H.O. and Mickelson, J.R. (2008) Glycogen synthase (GYS1) mutation causes a novel skeletal muscle glycogenosis. *Genomics*, **91**, 458–466.
- Pederson, B.A., Schroeder, J.M., Parker, G.E., Smith, M.W., DePaoli-Roach, A.A. and Roach, P.J. (2005) Glucose metabolism in mice lacking muscle glycogen synthase. *Diabetes*, **54**, 3466–3473.
- Irimia, J.M., Meyer, C.M., Peper, C.L., Zhai, L., Bock, C.B., Previs, S.F., McGuinness, O.P., DePaoli-Roach, A. and Roach, P.J. (2010) Impaired glucose tolerance and predisposition to the fasted state in liver glycogen synthase knock-out mice. *J. Biol. Chem.*, **285**, 12851–12861.
- Bao, Y., Kishnani, P., Wu, J.Y. and Chen, Y.T. (1996) Hepatic and neuromuscular forms of glycogen storage disease type IV caused by mutations in the same glycogen-branching enzyme gene. *J. Clin. Invest.*, **97**, 941–948.
- Ubogu, E.E., Hong, S.T., Akman, H.O., Dimauro, S., Katirji, B., Preston, D.C. and Shapiro, B.E. (2005) Adult polyglucosan body disease: a case report of a manifesting heterozygote. *Muscle Nerve*, **32**, 675–681.
- David, J.P., Ghazali, F., Fallet-Bianco, C., Wattez, A., Delaine, S., Boniface, B., Di Menza, C. and Delacourte, A. (1997) Glial reaction in the hippocampal formation is highly correlated with aging in human brain. *Neurosci. Lett.*, **235**, 53–56.
- Hansen, L.A., Armstrong, D.M. and Terry, R.D. (1987) An immunohistochemical quantification of fibrous astrocytes in the aging human cerebral cortex. *Neurobiol. Aging*, **8**, 1–6.

25. Kohama, S.G., Goss, J.R., Finch, C.E. and McNeill, T.H. (1995) Increases of glial fibrillary acidic protein in the aging female mouse brain. *Neurobiol. Aging*, **16**, 59–67.
26. Wierzbicka-Bobrowicz, T., Lewandowska, E., Stepien, T. and Modzelewska, J. (2008) Immunohistochemical and ultrastructural changes in the brain in probable adult glycogenosis type IV: adult polyglucosan body disease. *Folia Neuropathol.*, **46**, 165–175.
27. Ianzano, L., Zhang, J., Chan, E.M., Zhao, X.C., Lohi, H., Scherer, S.W. and Minassian, B.A. (2005) Lafora progressive myoclonus epilepsy mutation database-EPM2A and NHLRC1 (EPM2B) genes. *Hum. Mutat.*, **26**, 397.
28. Chan, E.M., Omer, S., Ahmed, M., Bridges, L.R., Bennett, C., Scherer, S.W. and Minassian, B.A. (2004) Progressive myoclonus epilepsy with polyglucosans (Lafora disease): evidence for a third locus. *Neurology*, **63**, 565–567.
29. Minassian, B.A., Lee, J.R., Herbrick, J.A., Huizenga, J., Soder, S., Mungall, A.J., Dunham, I., Gardner, R., Fong, C.Y., Carpenter, S. *et al.* (1998) Mutations in a gene encoding a novel protein tyrosine phosphatase cause progressive myoclonus epilepsy. *Nat. Genet.*, **20**, 171–174.
30. Ganesh, S., Delgado-Escueta, A.V., Sakamoto, T., Avila, M.R., Machado-Salas, J., Hoshii, Y., Akagi, T., Gomi, H., Suzuki, T., Amano, K. *et al.* (2002) Targeted disruption of the Epm2a gene causes formation of Lafora inclusion bodies, neurodegeneration, ataxia, myoclonus epilepsy and impaired behavioral response in mice. *Hum. Mol. Genet.*, **11**, 1251–1262.
31. Ianzano, L., Young, E.J., Zhao, X.C., Chan, E.M., Rodriguez, M.T., Torrado, M.V., Scherer, S.W. and Minassian, B.A. (2004) Loss of function of the cytoplasmic isoform of the protein laforin (EPM2A) causes Lafora progressive myoclonus epilepsy. *Hum. Mutat.*, **23**, 170–176.
32. Tagliabracci, V.S. and Roach, P.J. (2010) Insights into the mechanism of polysaccharide dephosphorylation by a glucan phosphatase. *Proc. Natl Acad. Sci. USA*, **107**, 15312–15313.
33. Pederson, B.A., Chen, H., Schroeder, J.M., Shou, W., DePaoli-Roach, A.A. and Roach, P.J. (2004) Abnormal cardiac development in the absence of heart glycogen. *Mol. Cell Biol.*, **24**, 7179–7187.